

Published in final edited form as:

Matrix Biol. 2009 April ; 28(3): 129–136. doi:10.1016/j.matbio.2009.01.005.

## Genetic evidence for key roles of decorin and biglycan in dentin mineralization

Naoto Haruyama<sup>1,\*,†</sup>, Taduru L. Sreenath<sup>1,\*</sup>, Shigeki Suzuki<sup>1</sup>, Xiaomei Yao<sup>3</sup>, Zhigang Wang<sup>3</sup>, Yong Wang<sup>3</sup>, Cherlita Honeycutt<sup>1</sup>, Renato V. Iozzo<sup>4</sup>, Marian F. Young<sup>2</sup>, and Ashok B. Kulkarni<sup>1</sup>

<sup>1</sup> Functional Genomics Section, Laboratory of Cell and Developmental Biology, Bethesda, MD, USA

<sup>2</sup> Molecular Biology of Bones and Teeth Section, Craniofacial and Skeletal Diseases Branch, National Institute of Dental and Craniofacial Research, National Institutes of Health, Department of Health and Human Services, Bethesda, MD, USA

<sup>3</sup> Department of Oral Biology, School of Dentistry, University of Missouri-Kansas City, MO, USA

<sup>4</sup> Department of Pathology, Anatomy, and Cell Biology, and the Kimmel Cancer Center, Thomas Jefferson University, Philadelphia, PA, USA

### Abstract

Targeted disruption of the dentin sialophosphoprotein (DSPP) gene in the mice (*Dspp*<sup>-/-</sup>) results in dentin mineralization defects with enlarged predentin phenotype similar to human dentinogenesis imperfecta type III. Using DSPP/biglycan (*Dspp*<sup>-/-</sup>*Bgn*<sup>-/0</sup>) and DSPP/decorin (*Dspp*<sup>-/-</sup>*Dcn*<sup>-/-</sup>) double knockout mice, here we determined that the enlarged predentin layer in *Dspp*<sup>-/-</sup> is rescued in the absence of decorin, but not in the absence of biglycan. However, Fourier transform infrared (FTIR) spectroscopy analysis reveals similar hypomineralization of dentin in both *Dspp*<sup>-/-</sup>*Bgn*<sup>-/0</sup> and *Dspp*<sup>-/-</sup>*Dcn*<sup>-/-</sup> teeth. Atomic force microscopy (AFM) analysis of collagen fibrils in dentin shows subtle differences in the collagen fibril morphology of these genotypes. The reduction of enlarged predentin in *Dspp*<sup>-/-</sup>*Dcn*<sup>-/-</sup> suggests that the elevated level of decorin in *Dspp*<sup>-/-</sup> predentin interferes with the mineralization process at the dentin mineralization front. On the other hand, the lack of DSPP and biglycan leads to the increased number of calcospherites in *Dspp*<sup>-/-</sup>*Bgn*<sup>-/0</sup> predentin, suggesting that a failure in coalescence of calcospherites was augmented in *Dspp*<sup>-/-</sup>*Bgn*<sup>-/0</sup> as compared to *Dspp*<sup>-/-</sup> teeth. These findings indicate that normal expression of small leucine rich proteoglycans, such as biglycan and decorin, plays an important role in the highly orchestrated process of dentin mineralization.

### Keywords

dentin sialophosphoprotein (DSPP); biglycan; decorin; knockout mouse; dentin mineralization; and dentinogenesis imperfecta (DGI)

---

Corresponding author: Functional Genomics Section, LCDB, NIDCR, NIH, 30 Convent Dr., MSC 4395, Bethesda, MD, USA 20892, Phone: 301-435-2887, FAX: 301-435-2888, E-mail address: E-mail: ak40m@nih.gov (A.B. Kulkarni).

\*N. Haruyama and T.L. Sreenath contributed equally to this work.

†Current address: Tohoku University Graduate School of Dentistry, Sendai, Japan

**Publisher's Disclaimer:** This is a PDF file of an unedited manuscript that has been accepted for publication. As a service to our customers we are providing this early version of the manuscript. The manuscript will undergo copyediting, typesetting, and review of the resulting proof before it is published in its final citable form. Please note that during the production process errors may be discovered which could affect the content, and all legal disclaimers that apply to the journal pertain.

## 1. Introduction

Over the past decade, significant progress has been made to further our understanding of non-collagenous proteins in dentin matrix. Indeed, dentin contains relatively unique non-collagenous extracellular matrix proteins, such as members of the SIBLING (small integrin-binding ligand glycoprotein) (Fisher *et al.*, 2003) and SLRPs (small leucine-rich repeat proteoglycans) families (Iozzo, 1997). These proteins are mainly secreted by odontoblasts (Embery *et al.*, 2001). The SIBLING family of secreted glycoprophosphoproteins includes bone sialoprotein (BSP), dentin matrix protein-1 (DMP1), osteopontin (OPN), matrix extracellular phosphoglycoprotein (MEPE), and dentin sialophosphoprotein (DSPP) (Fisher *et al.*, 2003; Fisher *et al.*, 2001).

DSPP, a highly acidic phosphorylated protein, is the major non-collagenous ECM in dentin. The *Dspp* gene, harboring five exons, is located among the SIBLING gene family cluster on mouse chromosome 5 (human chromosome 4) (Feng *et al.*, 1998; MacDougall, 2003; MacDougall *et al.*, 2006; Qin *et al.*, 2004). The DSPP protein, encoded from 4.4 kb mRNA, is believed to be cleaved into dentin sialoprotein (DSP) and dentin phosphoprotein (DPP; also known as phosphophoryn) (MacDougall *et al.*, 1997). A third portion of cleaved proteins, dentin glycoprotein (DGP), has been recently identified in the pig (Yamakoshi *et al.*, 2005). The targeted disruption of the *Dspp* gene in mice (*Dspp*<sup>-/-</sup> mouse) showed a tooth phenotype similar to that observed in dentinogenesis imperfecta type III (DGI-III) patients (OMIM#125500), including enlarged pulp chambers, increased width of predentin and dentin hypomineralization (Sreenath *et al.*, 2003). However, the precise roles of DSP and DPP are not fully understood. We earlier found that the *Dspp*<sup>-/-</sup> mouse had an increased deposition of two SLRPs, biglycan (BGN) and decorin (DCN), in the predentin zone, suggesting that the increased levels of biglycan or decorin may be the cause or consequence of hypomineralization and widened predentin in *Dspp*<sup>-/-</sup> mice (Sreenath *et al.*, 2003).

The members of the SLRP family have core proteins of about 40 kDa, that are dominated by a central domain composed of 6–10 tandemly repeated leucine rich sequences, and characteristics N- and C-terminal domains (Iozzo, 1999). Recent analysis of SLRP family encompasses now 5 classes with 17 distinct genes involved in a variety of cellular functions and signaling (Schaefer *et al.*, 2008). Biglycan (Fisher *et al.*, 1989) and decorin (Krusius *et al.*, 1986) are the closest members of class I SLRPs. Biglycan and decorin are widely distributed in mammalian tissues, including mineralized tissues such as bone and teeth (Hocking *et al.*, 1998; Iozzo *et al.*, 1996; Reed *et al.*, 2002). The N-terminal regions of decorin and biglycan are substituted with one and two chondroitin-sulfate (CS)/dermatan-sulfate (DS) glycosaminoglycans (GAGs) chains, respectively (Embery *et al.*, 2001). The SLRPs, especially decorin, appear to interact with collagen through the binding with the leucine rich region of the protein core (Weber *et al.*, 1996), which can modify the deposition and arrangement of collagen fibrils in the ECMs of soft tissues (Danielson *et al.*, 1997). In addition to modifying the extracellular environment, interactions of SLRPs with cells, and with growth factors such as transforming growth factor- $\beta$  (TGF- $\beta$ ) affect the proliferation of cells (Ferdous *et al.*, 2007; Kresse *et al.*, 2001; Markmann *et al.*, 2000).

To delineate the precise functions of biglycan and decorin in dentin defects observed in *Dspp*<sup>-/-</sup> mice, we generated and analyzed DSPP/biglycan and DSPP/Decorin double knock out (KO) mice (*Dspp*<sup>-/-</sup>*Bgn*<sup>-/-</sup> and *Dspp*<sup>-/-</sup>*Dcn*<sup>-/-</sup>). Our findings here show that the elevated decorin expression is one of the major causative factors of the enlarged predentin phenotype in *Dspp*<sup>-/-</sup> mouse teeth.

## 2. Results

### 2.1. Biglycan and decorin expression in $Dspp^{-/-}Bgn^{-/0}$ or $Dspp^{-/-}Dcn^{-/-}$ mouse incisors

After the serial mating of progeny from  $Dspp^{-/-} \times Bgn^{-/0}$  and  $Dspp^{-/-} \times Dcn^{-/-}$ , the successful generation of  $Dspp^{-/-}Bgn^{-/0}$  or  $Dspp^{-/-}Dcn^{-/-}$  mice was confirmed by genotyping using PCR (data not shown), and also by immunostaining of tooth sections using anti-BGN or anti-DCN specific antibodies (Fig. 1). No positive staining for biglycan or decorin could be detected in  $Dspp^{-/-}Bgn^{-/0}$  or  $Dspp^{-/-}Dcn^{-/-}$  incisors, respectively (Fig. 1 C and H). In *WT* incisors, biglycan and decorin were predominantly distributed in a thin predentin layer (Fig. 1 A and E; black arrows) and odontoblasts (Fig. 1 A and E; red arrows). The biglycan and decorin were also localized in  $Dspp^{-/-}$  widened predentin (Fig. 1 B and F; black arrows) and in odontoblasts (Fig. 1 B and F; red arrows) as previously reported (Sreenath *et al.*, 2003). The biglycan and decorin staining was barely visible in the mineralized dentin region of all the genotypes. Notably, the widened predentin zone in  $Dspp^{-/-}Bgn^{-/0}$  exhibited a strong immunostaining for decorin (Fig. 1G, arrow). The  $Dspp^{-/-}Dcn^{-/-}$  incisor showed biglycan staining in the thin predentin layer (Fig. 1D, arrow).

### 2.2. Decorin deficiency in the $Dspp^{-/-}$ mice rescues the widened-predentin phenotype, while biglycan deficiency displays an increased number of calcospherites at the mineralization front in the $Dspp^{-/-}$ mice

Histological analysis of *WT*,  $Dspp^{-/-}$ ,  $Dspp^{-/-}Bgn^{-/0}$  and  $Dspp^{-/-}Dcn^{-/-}$  incisors was performed by H&E staining (Fig. 2). The dentin in  $Dspp^{-/-}$ ,  $Dspp^{-/-}Bgn^{-/0}$  and  $Dspp^{-/-}Dcn^{-/-}$  incisors was eosinophilic, whereas the *WT* incisor showed hematoxyphil dentin with a more intense purple color. In the *WT* incisor, the thick dentin and thin predentin (black arrows), lined by an odontoblast layer, surrounded the tooth pulp (Fig. 2A and E). As previously reported,  $Dspp^{-/-}$  mice showed increased width of predentin with pale pink color (Fig. 2B and 2F, asterisk). The predentin in  $Dspp^{-/-}$  mice displayed an increased number of calcospherites (globular dentin) formed at the mineralization front, as compared to *WT* (Fig. 2F, red arrows). In the  $Dspp^{-/-}Bgn^{-/0}$  incisor, the predentin width remained widened with a concurrent increase in the number of calcospherites, resulting in the irregular mineralization front (Fig. 2C and G, asterisk and red arrows). However, the lack of decorin in the DSPP null background significantly rescued the widened predentin phenotype observed in the  $Dspp^{-/-}$  incisor (Fig. 1 D and H, black arrows).

### 2.3. Dentin hypomineralization in $Dspp^{-/-}$ mice remains unchanged by the deficiency of decorin or biglycan

To compare the differences in dentin mineralization among the four different genotypes, the incisors were examined by microradiography (Fig. 3). The X-ray opacities of dentin at the labiolingual middle area (pointed in Fig. 3A, asterisk) appeared to be decreased in  $Dspp^{-/-}$  mice (Fig. 3B), as compared to X-ray opacities in *WT* mice. The opacity in  $Dspp^{-/-}Bgn^{-/0}$  incisor looked strikingly decreased (Fig. 3C), whereas the  $Dspp^{-/-}Dcn^{-/-}$  incisor demonstrated the increased opacity (Fig. 3D) as compared with the  $Dspp^{-/-}$  incisor (representative graph shown in Fig. 3E). To further analyze and compare the differences in mineralization at the ultra-structural level, the incisors were examined by scanning electron microscopy (SEM) (Fig. 4A–D). The fractured surface characteristics of the *WT* incisor indicated a compact and mineralized dentin. Compared to the *WT* incisors, the collagen fibrils were clearly seen in the fractured dentin surface of the  $Dspp^{-/-}$  incisors (Fig. 4A and B). Collagen fibrils were also observed in the dentinal tubules and intertubular dentin of  $Dspp^{-/-}Bgn^{-/0}$  and  $Dspp^{-/-}Dcn^{-/-}$  incisors (Fig. 4C and D), but there were far fewer than the amount seen in  $Dspp^{-/-}$  incisors. Quantitative analysis by Fourier transform infrared (FTIR) spectroscopy was also performed to compare the mineral contents (mineral to matrix ratio) in dentin (Fig. 4E). The  $Dspp^{-/-}$ ,  $Dspp^{-/-}Bgn^{-/0}$  and  $Dspp^{-/-}Dcn^{-/-}$  mice had significantly lower mineral contents in dentin as

compared to those in *WT* mice. The *Dspp*<sup>-/-</sup> dentin had the lowest mineral contents among the three knockout mice groups. The mean values of mineral content in *Dspp*<sup>-/-</sup>*Bgn*<sup>-/0</sup> and *Dspp*<sup>-/-</sup>*Dcn*<sup>-/-</sup> were larger than those in the *Dspp*<sup>-/-</sup>, but not statistically significant.

#### 2.4. Ultrastructural changes of dentin collagen fibrils in *Dspp*<sup>-/-</sup>, *Dspp*<sup>-/-</sup>*Bgn*<sup>-/0</sup> and *Dspp*<sup>-/-</sup>*Dcn*<sup>-/-</sup> examined by atomic force microscopy (AFM)

The fractured surfaces of dentin specimens treated by EDTA were used to examine the collagen fibrils by AFM (Fig. 5). After a 3-min 0.5 M EDTA treatment, the collagen fibril structures could not be observed in *WT* samples because of insufficient decalcification with EDTA (data not shown). With a 5-min 0.5 M EDTA treatment, D-structure (periodicity of the gap zone) was clearly observed (Fig. 5A) in collagen fibrils. In *Dspp*<sup>-/-</sup> samples treated by 0.5M EDTA for 3 min, the collagen fibrils and the D-structure could be observed by AFM (Fig. 5B). After a 3-min treatment with EDTA, *Dspp*<sup>-/-</sup>*Bgn*<sup>-/0</sup> and *Dspp*<sup>-/-</sup>*Dcn*<sup>-/-</sup> samples also showed the clear collagen fibrils, exposed due to the removal of mineralized material (Fig. 5C and D). The periodicity of the D-structures in *Dspp*<sup>-/-</sup> collagen fibrils was significantly shorter than that of the *Dspp*<sup>-/-</sup>*Bgn*<sup>-/0</sup> or *Dspp*<sup>-/-</sup>*Dcn*<sup>-/-</sup> collagen fibrils (Fig. 5E). Although there was no significant difference in the mean values of collagen fibril diameters among the four genotypes, the standard deviations in fibril diameter were bigger in the *Dspp*<sup>-/-</sup> (94.0 ± 20.9) and *Dspp*<sup>-/-</sup>*Dcn*<sup>-/-</sup> (107 ± 21.8) incisors (Fig. 5F) as compared with the *WT* (100.2 ± 6.8) and *Dspp*<sup>-/-</sup>*Bgn*<sup>-/0</sup> (95.7 ± 7.0).

### 3. Discussion

The non-collagenous ECM proteins are believed to play important roles in the biomineralization process that forms hard tissues. In order to characterize the biological roles played by biglycan and decorin in the *Dspp*<sup>-/-</sup> teeth, we selectively bred mice to generate deficiency of either biglycan or decorin in the DSPP null background. The width of predentin was almost restored to a normal width in the *Dspp*<sup>-/-</sup>*Dcn*<sup>-/-</sup>. In contrast, not only the predentin remained widened, but increase in calcospherites was also observed in *Dspp*<sup>-/-</sup>*Bgn*<sup>-/0</sup> teeth. These results suggest that the widened predentin in *Dspp*<sup>-/-</sup> teeth was most likely due to the increased level of decorin in *Dspp*<sup>-/-</sup> predentin. In other words, the excess decorin, but not biglycan was responsible for inhibiting conversion of predentin to dentin at the mineralization front in *Dspp*<sup>-/-</sup> mice. The excess biglycan may have a positive effect on the coalescence of calcospherites in *Dspp*<sup>-/-</sup> mice to a certain extent, but cannot compensate for the failure in predentin/dentin conversion possibly due to the excess decorin.

First, we compared the histological differences in the incisors from four different mouse groups. The dentin in *WT* was stained relatively purple, whereas the genotypes which lacked DSPP displayed the pale pink-colored dentin layers (Fig. 2). DSPP is not only a highly phosphorylated acidic protein, but it is also the most abundant non-collagenous protein in dentin. Particularly, the acidic peptide: DPP is present only in the mineralized matrices of primary dentin (Rahima *et al.*, 1988). Because the cationic or basic dye such as hematoxylin has an affinity for the tissue with a net negative charge, the removal of phosphate groups might have led to the striking color difference in DSPP null teeth as shown in the H&E staining.

It has been reported that the addition of biglycan increased apatite formation *in vitro*, suggesting the potential role of biglycan as a nucleator of mineralization (Boskey *et al.*, 1997). Interestingly, the number of calcospherites in the dentin of *Dspp*<sup>-/-</sup>*Bgn*<sup>-/0</sup> increased, compared to that of *Dspp*<sup>-/-</sup>. The irregularity of mineralization front appeared to be much more increased in *Dspp*<sup>-/-</sup>*Bgn*<sup>-/0</sup> (Fig. 2C and G), suggesting that the coalescence of calcospherites was severely reduced in *Dspp*<sup>-/-</sup>*Bgn*<sup>-/0</sup> dentin. On the other hand, the width of the predentin layer in *Dspp*<sup>-/-</sup>*Dcn*<sup>-/-</sup> incisors dramatically decreased as compared to *Dspp*<sup>-/-</sup>, and no (or dramatically fewer) calcospherites were observed, indicating that removing of decorin induces

the predentin-dentin conversion in *Dspp*<sup>-/-</sup> teeth. These results suggest that the conversion of predentin to dentin at the mineralization front in *Dspp*<sup>-/-</sup> mice is regulated positively by biglycan but negatively by decorin.

Both biglycan and decorin single gene knockout mice exhibited altered numbers of collagen fibrils in the molar predentin at a younger age (Goldberg *et al.*, 2005). Type I collagen is secreted by odontoblasts into predentin and then recruited into the mineralization front as bundles of collagen fibrils, thus forming mineralized dentin. Both biglycan and decorin are known to interact with type I collagen fibrils (Schonherr *et al.*, 1995; Weber *et al.*, 1996). Decorin in particular binds to the gap (also referred as 'D') region in the collagen fibril, which is believed to block initiation of mineralization (Hoshi *et al.*, 1999). *In vitro* experiments have also shown such inhibitory functions of proteoglycans in mineralization (Chen *et al.*, 1985). Because the localization of proteoglycans might be one of the key factors in the mineralization process, we hypothesized that the increased decorin protein levels, due to either enhanced expression or decreased degradation, may be one of the key factors which causes widening of the predentin zone observed in *Dspp*<sup>-/-</sup> mice. We have previously demonstrated that expression of MMP-3, one of the major proteases that degrades decorin, remains unchanged in *Dspp*<sup>-/-</sup> mice (Sreenath *et al.*, 2003), suggesting that the increased expression of decorin prevents recruitment of collagen fibrils during developmental mineralization, which resulted in widened predentin.

It has also been reported that the biglycan single knockout mice did not show any dentin defect in incisors, whereas the mineralization defects found in developing stages of molars were eventually recovered by 6-weeks-old (Goldberg *et al.*, 2005). The decorin single knockout mice also showed that the dentin in 1-day-old molars was porous and poorly mineralized, although the severe mineralization defects were recovered by 6-weeks-old (Goldberg *et al.*, 2005). In this study, we compared the mineralization of biglycan or decorin null teeth with DSPP null background. The microradiographs in Fig. 3 showed that the opacity in the *Dspp*<sup>-/-</sup>*Bgn*<sup>-/0</sup> incisor was strikingly decreased, whereas in the *Dspp*<sup>-/-</sup>*Dcn*<sup>-/-</sup>, the opacity was increased in comparison to that of the *Dspp*<sup>-/-</sup> incisor. However, it is conceivable that the thickness ratio between the unmineralized predentin and the mineralized dentin was essential for the altered X-ray opacities observed in the dentin specimens, since the total thickness of predentin and dentin did not seem to be altered between genotypes. To investigate the quality of dentin mineralization, we conducted further observations using SEM and FTIR spectroscopy. Interestingly, dentin hypomineralization appeared to be partially rescued by removing the biglycan or decorin from *Dspp*<sup>-/-</sup> mice based on the SEM observation (Fig. 4A–D). However, as shown in Fig. 4E, the quantitative analysis by FTIR used to determine the differences between mineral contents did not show significant changes in *Dspp*<sup>-/-</sup>, *Dspp*<sup>-/-</sup>*Bgn*<sup>-/0</sup> and *Dspp*<sup>-/-</sup>*Dcn*<sup>-/-</sup> dentin. These results suggest that the thickness of mineralized dentin, but not predentin, primarily contributed to the X-ray opacity of dentin, and the ablation of biglycan or decorin may not significantly affect the quality of dentin mineralization in a DSPP null background. In other words, the lack of DSPP could be the causative factor for the hypomineralization of dentin in *Dspp*<sup>-/-</sup>, *Dspp*<sup>-/-</sup>*Bgn*<sup>-/0</sup> and *Dspp*<sup>-/-</sup>*Dcn*<sup>-/-</sup> mice.

We further examined the incisor samples by AFM in order to investigate whether the altered collagen fibrillogenesis or microstructures affect the mineralization in dentin. The typical 60–70nm D-periodicity of the type I collagen was observed in the all genotypes. Although the periodicity of the D-structures in the *Dspp*<sup>-/-</sup> incisor was significantly shorter than that of the *Dspp*<sup>-/-</sup>*Bgn*<sup>-/0</sup> or *Dspp*<sup>-/-</sup>*Dcn*<sup>-/-</sup> incisors (Fig. 5E), the functional significance of the difference in D-periods could not be determined from our results on dentin mineralization. The difference might simply reflect the change in the susceptibility of tissue shrinkage to the chemical fixation and hydration of the specimens. However, the gap (D zone) regions of type



I collagen are considered to be the crystal nucleation sites in biomineralization (Tong *et al.*, 2003). The question of whether the D-periodicity would affect the tissue mineralization remains entirely open-ended. We also demonstrated that there is no significant difference in the mean values of collagen fibril diameter among all four genotypes. However, the standard deviations in fibril diameters were bigger in the *Dspp*<sup>-/-</sup> and *Dspp*<sup>-/-</sup>*Dcn*<sup>-/-</sup> incisors (Fig. 5F). The variation in fibril diameter apparent in the *Dspp*<sup>-/-</sup>*Dcn*<sup>-/-</sup> incisor was consistent with one of the key roles of decorin in regulating collagen fibrillogenesis both *in vivo* and *in vitro* (Reed *et al.*, 2002). Although the collagen organization and bundles seemed normal (Sreenath *et al.*, 2003), the collagen fibrils with un-uniform diameters may have been present in the collagen bundles of *Dspp*<sup>-/-</sup> dentin. Because the microstructures of collagen fibrils and the initiation of dentin mineralization did not show any relationship to one another, the role of biglycan and decorin in the initial mineralization of *Dspp*<sup>-/-</sup> dentin might not be acting through the regulation of collagen fibrillogenesis, but perhaps acting through the regulation of key signaling pathways involved in dentin mineralization.

It would be necessary to further investigate the mechanisms of how the deletion of DSPP positively regulates the expression of biglycan and decorin in odontoblasts. So far, several mutations in the *DSPP* gene are reported in DGI and DD patients. However, it is well-known that the severity of dentin defect is not correlated with the mutation point, indicating that there are other factors involved in this disease (McKnight *et al.*, 2008b). Biglycan and decorin may be the major candidates for what factors affect these severities, since they seem to act more drastically in DSPP null background than in their single knockout. Most of the *DSPP* mutations observed in DGI and DD patients are predicted to result in accumulation of mutated DSPP protein in rough endoplasmic reticulum (rER) (McKnight *et al.*, 2008a), which may affect the secretion of dentin ECM proteins. Thus, the secretion levels or patterns of biglycan and decorin might affect each individual patient differently, leading to the variety of this disease.

In summary, our genetic studies reveal that increased levels of decorin in pre-dentin of *Dspp*<sup>-/-</sup> is associated with a widened pre-dentin phenotype that resembles DGI III. Most importantly, our findings highlight the importance of SLRPs in dentin mineralization.

## 4. Experimental procedures

### 4.1. Animals

*Dspp*, *Bgn*, and *Dcn* knockout mice were generated as reported previously (Danielson *et al.*, 1997; Sreenath *et al.*, 2003; Xu *et al.*, 1998). *Dspp*<sup>-/-</sup>*Bgn*<sup>-/-</sup> and *Dspp*<sup>-/-</sup>*Dcn*<sup>-/-</sup> mice were generated by sequential breeding of *Dspp*<sup>-/-</sup> with *Bgn*<sup>-/-</sup> or *Dcn*<sup>-/-</sup> mice. The genotyping of WT (*Dspp*<sup>+/+</sup>*Bgn*<sup>+/+</sup>*Dcn*<sup>+/+</sup>), *Dspp*<sup>-/-</sup>, *Dspp*<sup>-/-</sup>*Bgn*<sup>-/-</sup> and *Dspp*<sup>-/-</sup>*Dcn*<sup>-/-</sup> mice was determined by polymerase chain reaction (PCR) as described previously (Bi *et al.*, 2005; Sreenath *et al.*, 2003). Standard NIH guidelines were followed to house, feed and breed the mice. These studies were carried out with the approval of the institutional animal committee.

### 4.2. Tissue sample preparation, histology and immunohistochemistry

All incisor samples were collected from 6-month-old null and WT control mice. After the mandible and maxilla were dissected, the jaws, including teeth, were fixed in 4% paraformaldehyde (PFA) overnight. For histological analysis, the samples were decalcified in 0.1M ethylene diamine tetra-acetic acid (EDTA) in phosphate-buffered saline (PBS), and embedded in paraffin. For the microradiography, scanning electron microscopy (SEM), Fourier transform infrared (FTIR) spectroscopy and atomic force microscopy (AFM) analysis, the skin and muscles from the heads of the mice were dissected. The brain was also excluded to allow for better diffusion of the fixative solution (2.5% glutaraldehyde and 2.0% paraformaldehyde,

in 0.1 M cacodylate buffer, pH 7.2) for 2 hrs. The skulls were later rinsed in the fixative solution and stored at room temperature for 24 hrs. Five micrometer-thick tissue sections were prepared from paraffin blocks for histology. Only the sections at the cervical level (tooth erupting area) were used as incisor samples. Hematoxylin and Eosin (H&E) staining was performed for general histology on the incisor samples. For the immunohistochemistry, the sections were dewaxed and treated with Peroxidase I (Biocare Medical Concord, CA) for 5 min at RT to inactivate endogenous peroxidase. Next, sections were blocked with Rodent Block M (Biocare Medical) for 30 min at RT, and then incubated with rabbit polyclonal anti-BGN (LF-159) (1:800), anti-DCN (LF-113) (1:800) (Fisher *et al.*, 1995) (kind gifts from Dr. Larry Fisher, NIDCR/NIH, Bethesda, MD) for 2h at RT. The immune complexes were incubated with Rodent HRP-Polymer (Biocare Medical) for 30 min, and the peroxidase reaction was visualized by a DAB (3, 3'-Diaminobenzidine) kit (Sigma). Nuclear counterstaining was performed using Hematoxylin for 5 seconds.

#### 4.3. Microradiography

The upper incisors were isolated from the skulls and radiographed using a Faxitron MX20 Specimen Radiography System (Faxitron X-ray Corp., Wheeling, IL) at energy settings 120 s at 15V (Sreenath *et al.*, 2003). The images were captured on X-OMAT TL film (Eastman Kodak, Rochester, NY), and then scanned using a computerized image analysis system. The mean gray values of incisors were measured by Image J (<http://rsbweb.nih.gov/ij/>) to assess the differences in the X-ray opacities.

#### 4.4. Fourier transform infrared (FTIR) spectroscopy

FTIR spectroscopy was performed in order to measure the *in situ* mineral to matrix ratio in dentin (Boskey *et al.*, 2003). In brief, the specimens were cut transversely at the erupting level of incisors and mounted on glass slides with the cut surface facing up. FTIR spectra were collected using the Perkin-Elmer Spotlight 300 micro-spectroscopy, coupled with a drop-down Ge ATR (attenuate total reflectance) accessory. Spectra were scanned between 4000 and 720  $\text{cm}^{-1}$  at a 4  $\text{cm}^{-1}$  spectral resolution, with 512 scans.

#### 4.5. Scanning electron microscopy (SEM) and atomic force microscopy (AFM) analysis

The incisors for SEM and AFM were fixed as described above, washed and dehydrated. After drying, the specimens were fractured at the erupting level of the incisors for the cross-sectional analysis, and mounted on aluminum stubs with the fractured surface facing upward to a stub. They were then examined using a FEI/Philips XL30 field emission environmental SEM (Philips, Eindhoven, Netherlands) at 5 kV. The other halves of the same specimens used for SEM observations were further treated with 0.5 M EDTA for either 3 or 5 minutes in order to examine collagen fibril diameters and banding structures by AFM. The AFM images were obtained using a Nanoscope IIIa scanning probe microscope (Digital Instruments, Veeco Metrology Group, Inc., Santa Barbara, CA) operated in contact mode under ambient conditions ( $24 \pm 2^\circ\text{C}$ ,  $40 \pm 5\%$  Relative humidity). Silicon nitride cantilevers (NP-S, Veeco Metrology Group) with a spring constant of approximately 0.06 N/m were used. The diameters and D-structures of collagen fibrils were measured using cross-sectional analysis with Nanoscope software 5.30 version (DI-Veeco, Santa Barbara, CA).

#### 4.6. Statistical analysis

All the graphs are expressed as means  $\pm$  SD. The data were subjected to one-way analysis of variance (ANOVA) followed by the Tukey's test to identify differences between groups, except for the data in Fig. 3E.

## Acknowledgements

We would like to acknowledge Dr. Changqi Xu for the AFM data analysis. We would like to thank Harry Grant for the editorial assistance. These studies were supported by the Intramural Division of National Institute of Dental and Craniofacial Research.

## References

- Bi Y, Stuelten CH, Kilts T, Wadhwa S, Iozzo RV, Robey PG, Chen XD, Young MF. Extracellular matrix proteoglycans control the fate of bone marrow stromal cells. *J Biol Chem* 2005;280:30481–30489. [PubMed: 15964849]
- Boskey AL, Moore DJ, Amling M, Canalis E, Delany AM. Infrared analysis of the mineral and matrix in bones of osteonectin-null mice and their wildtype controls. *J Bone Miner Res* 2003;18:1005–1011. [PubMed: 12817752]
- Boskey AL, Spevak L, Doty SB, Rosenberg L. Effects of bone CS-proteoglycans, DS-decorin, and DS-biglycan on hydroxyapatite formation in a gelatin gel. *Calcif Tissue Int* 1997;61:298–305. [PubMed: 9312200]
- Chen CC, Boskey AL. Mechanisms of proteoglycan inhibition of hydroxyapatite growth. *Calcif Tissue Int* 1985;37:395–400. [PubMed: 2412669]
- Danielson KG, Baribault H, Holmes DF, Graham H, Kadler KE, Iozzo RV. Targeted disruption of decorin leads to abnormal collagen fibril morphology and skin fragility. *J Cell Biol* 1997;136:729–743. [PubMed: 9024701]
- Embery G, Hall R, Waddington R, Septier D, Goldberg M. Proteoglycans in dentinogenesis. *Crit Rev Oral Biol Med* 2001;12:331–349. [PubMed: 11603505]
- Feng JQ, Luan X, Wallace J, Jing D, Ohshima T, Kulkarni AB, D'Souza RN, Kozak CA, MacDougall M. Genomic organization, chromosomal mapping, and promoter analysis of the mouse dentin sialophosphoprotein (Dspp) gene, which codes for both dentin sialoprotein and dentin phosphoprotein. *J Biol Chem* 1998;273:9457–9464. [PubMed: 9545272]
- Ferdous Z, Wei VM, Iozzo R, Hook M, Grande-Allen KJ. Decorin-transforming growth factor-interaction regulates matrix organization and mechanical characteristics of three-dimensional collagen matrices. *J Biol Chem* 2007;282:35887–35898. [PubMed: 17942398]
- Fisher LW, Fedarko NS. Six genes expressed in bones and teeth encode the current members of the SIBLING family of proteins. *Connect Tissue Res* 2003;44(Suppl 1):33–40. [PubMed: 12952171]
- Fisher LW, Stubbs JT 3rd, Young MF. Antisera and cDNA probes to human and certain animal model bone matrix noncollagenous proteins. *Acta Orthop Scand Suppl* 1995;266:61–65. [PubMed: 8553864]
- Fisher LW, Termine JD, Young MF. Deduced protein sequence of bone small proteoglycan I (biglycan) shows homology with proteoglycan II (decorin) and several nonconnective tissue proteins in a variety of species. *J Biol Chem* 1989;264:4571–4576. [PubMed: 2647739]
- Fisher LW, Torchia DA, Fohr B, Young MF, Fedarko NS. Flexible structures of SIBLING proteins, bone sialoprotein, and osteopontin. *Biochem Biophys Res Commun* 2001;280:460–465. [PubMed: 11162539]
- Goldberg M, Septier D, Rapoport O, Iozzo RV, Young MF, Amey LG. Targeted disruption of two small leucine-rich proteoglycans, biglycan and decorin, excerpts divergent effects on enamel and dentin formation. *Calcif Tissue Int* 2005;77:297–310. [PubMed: 16283572]
- Hocking AM, Shinomura T, McQuillan DJ. Leucine-rich repeat glycoproteins of the extracellular matrix. *Matrix Biol* 1998;17:1–19. [PubMed: 9628249]
- Hoshi K, Kemmotsu S, Takeuchi Y, Amizuka N, Ozawa H. The primary calcification in bones follows removal of decorin and fusion of collagen fibrils. *J Bone Miner Res* 1999;14:273–280. [PubMed: 9933482]
- Iozzo RV. The family of the small leucine-rich proteoglycans: key regulators of matrix assembly and cellular growth. *Crit Rev Biochem Mol Biol* 1997;32:141–174. [PubMed: 9145286]
- Iozzo RV. The biology of the small leucine-rich proteoglycans. Functional network of interactive proteins. *J Biol Chem* 1999;274:18843–18846. [PubMed: 10383378]



- Iozzo RV, Murdoch AD. Proteoglycans of the extracellular environment: clues from the gene and protein side offer novel perspectives in molecular diversity and function. *Faseb J* 1996;10:598–614. [PubMed: 8621059]
- Kresse H, Schonherr E. Proteoglycans of the extracellular matrix and growth control. *J Cell Physiol* 2001;189:266–274. [PubMed: 11748584]
- Krusius T, Ruoslahti E. Primary structure of an extracellular matrix proteoglycan core protein deduced from cloned cDNA. *Proc Natl Acad Sci U S A* 1986;83:7683–7687. [PubMed: 3484330]
- MacDougall M. Dental structural diseases mapping to human chromosome 4q21. *Connect Tissue Res* 2003;44(Suppl 1):285–291. [PubMed: 12952210]
- MacDougall M, Dong J, Acevedo AC. Molecular basis of human dentin diseases. *Am J Med Genet A* 2006;140:2536–2546. [PubMed: 16955410]
- MacDougall M, Simmons D, Luan X, Nydegger J, Feng J, Gu TT. Dentin phosphoprotein and dentin sialoprotein are cleavage products expressed from a single transcript coded by a gene on human chromosome 4. Dentin phosphoprotein DNA sequence determination. *J Biol Chem* 1997;272:835–842. [PubMed: 8995371]
- Markmann A, Hausser H, Schonherr E, Kresse H. Influence of decorin expression on transforming growth factor-beta-mediated collagen gel retraction and biglycan induction. *Matrix Biol* 2000;19:631–636. [PubMed: 11102752]
- McKnight DA, Simmer JP, Hart PS, Hart TC, Fisher LW. Overlapping DSPP mutations cause dentin dysplasia and dentinogenesis imperfecta. *J Dent Res* 2008a;87:1108–1111. [PubMed: 19029076]
- McKnight DA, Suzanne Hart P, Hart TC, Hartsfield JK, Wilson A, Wright JT, Fisher LW. A comprehensive analysis of normal variation and disease-causing mutations in the human DSPP gene. *Hum Mutat* 2008b;29:1392–1404. [PubMed: 18521831]
- Qin C, Baba O, Butler WT. Post-translational modifications of sibling proteins and their roles in osteogenesis and dentinogenesis. *Crit Rev Oral Biol Med* 2004;15:126–136. [PubMed: 15187031]
- Rahima M, Tsay TG, Andujar M, Veis A. Localization of phosphophoryn in rat incisor dentin using immunocytochemical techniques. *J Histochem Cytochem* 1988;36:153–157. [PubMed: 3335773]
- Reed CC, Iozzo RV. The role of decorin in collagen fibrillogenesis and skin homeostasis. *Glycoconj J* 2002;19:249–255. [PubMed: 12975602]
- Schaefer L, Iozzo RV. Biological Functions of the Small Leucine-rich Proteoglycans: From Genetics to Signal Transduction. *J Biol Chem* 2008;283:21305–21309. [PubMed: 18463092]
- Schonherr E, Witsch-Prehm P, Harrach B, Robenek H, Rauterberg J, Kresse H. Interaction of biglycan with type I collagen. *J Biol Chem* 1995;270:2776–2783. [PubMed: 7852349]
- Sreenath T, Thyagarajan T, Hall B, Longenecker G, D'Souza R, Hong S, Wright JT, MacDougall M, Sauk J, Kulkarni AB. Dentin sialophosphoprotein knockout mouse teeth display widened predentin zone and develop defective dentin mineralization similar to human dentinogenesis imperfecta type III. *J Biol Chem* 2003;278:24874–24880. [PubMed: 12721295]
- Tong W, Glimcher MJ, Katz JL, Kuhn L, Eppell SJ. Size and shape of mineralites in young bovine bone measured by atomic force microscopy. *Calcif Tissue Int* 2003;72:592–598. [PubMed: 12724830]
- Weber IT, Harrison RW, Iozzo RV. Model structure of decorin and implications for collagen fibrillogenesis. *J Biol Chem* 1996;271:31767–31770. [PubMed: 8943211]
- Xu T, Bianco P, Fisher LW, Longenecker G, Smith E, Goldstein S, Bonadio J, Boskey A, Heegaard AM, Sommer B, Satomura K, Dominguez P, Zhao C, Kulkarni AB, Robey PG, Young MF. Targeted disruption of the biglycan gene leads to an osteoporosis-like phenotype in mice. *Nat Genet* 1998;20:78–82. [PubMed: 9731537]
- Yamakoshi Y, Hu JC, Fukae M, Zhang H, Simmer JP. Dentin glycoprotein: the protein in the middle of the dentin sialophosphoprotein chimera. *J Biol Chem* 2005;280:17472–17479. [PubMed: 15728577]

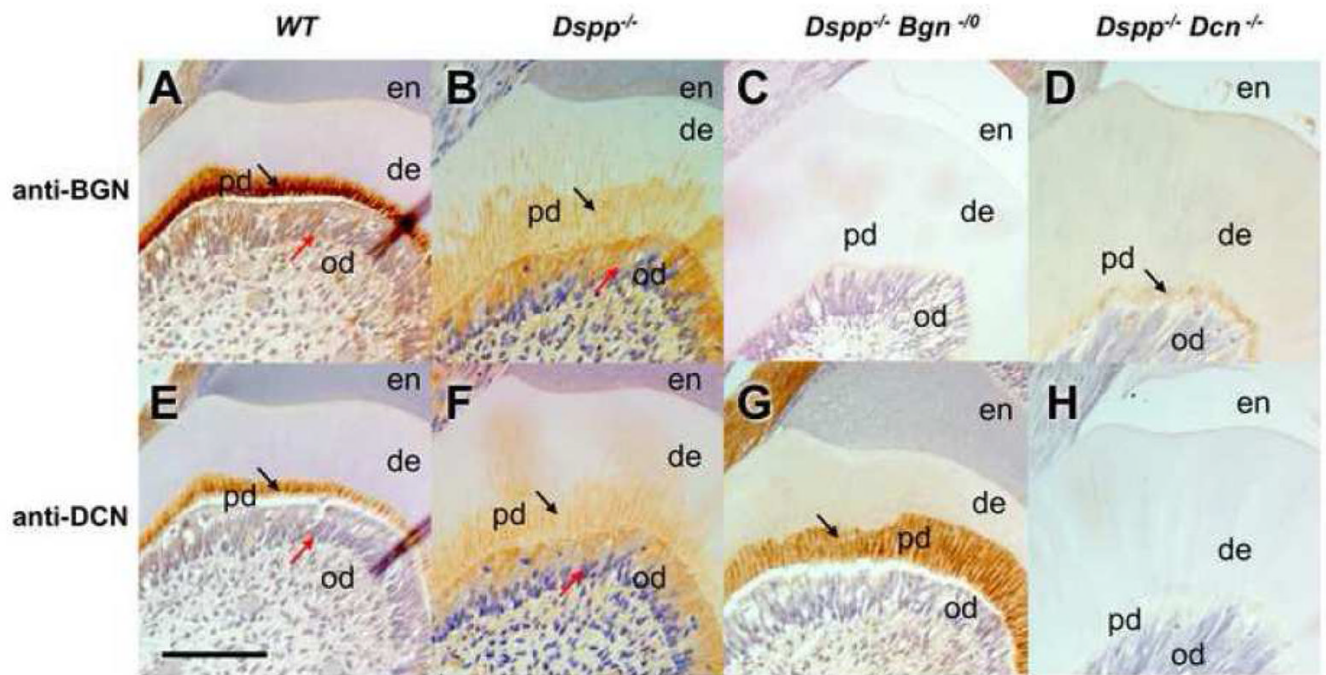


**Fig. 1. Localization of biglycan and decorin in *WT*, *Dspp*<sup>-/-</sup>, *Dspp*<sup>-/-</sup>*Bgn*<sup>-/-</sup>, and *Dspp*<sup>-/-</sup>*Dcn*<sup>-/-</sup> mice**

Immunostaining of 6-month-old incisors from *WT*, *Dspp*<sup>-/-</sup>, *Dspp*<sup>-/-</sup>*Bgn*<sup>-/-</sup>, and *Dspp*<sup>-/-</sup>*Dcn*<sup>-/-</sup> mice with anti-BGN or anti-DCN antibodies. In *WT*, biglycan and decorin were predominantly distributed in the narrow predentin (A and D; black arrows) and odontoblast cell bodies (A and D; red arrows). The biglycan and decorin were also localized in *Dspp*<sup>-/-</sup> widened predentin (Fig. 1 B and F; black arrows) and in odontoblasts (Fig. 1 B and F; red arrows) as previously reported. Biglycan or decorin could not be detected in *Dspp*<sup>-/-</sup>*Bgn*<sup>-/-</sup> (C) or *Dspp*<sup>-/-</sup>*Dcn*<sup>-/-</sup> incisor teeth (H), respectively. en, enamel; de, dentin; pd, predentin; od, odontoblasts. Bar = 100  $\mu$ m

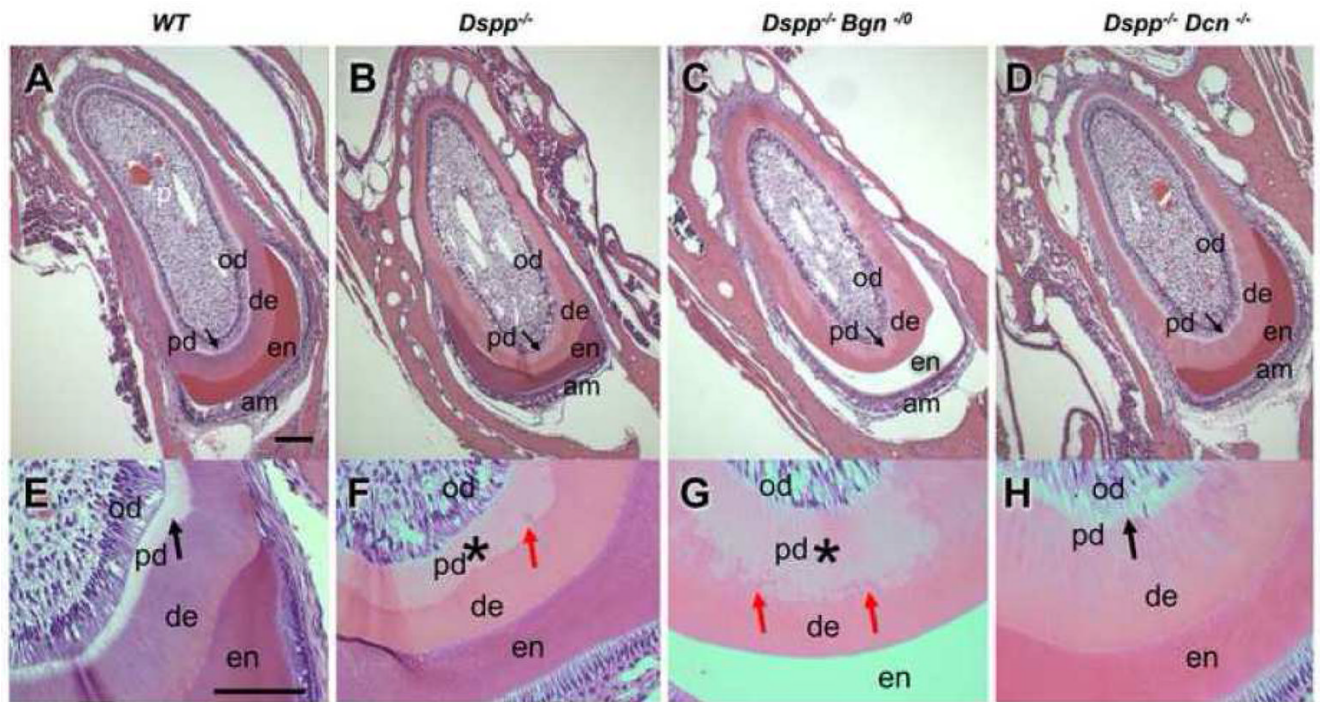


**Fig. 2. Widened predentin resembling dentinogenesis imperfecta in *Dspp*<sup>-/-</sup> null mice was reduced in thickness by removing decorin**

H&E stainings of 6-month-old incisors from *WT* (A and E), *Dspp*<sup>-/-</sup> (B and F), *Dspp*<sup>-/-</sup>*Bgn*<sup>-/-</sup> (C and G) and *Dspp*<sup>-/-</sup>*Dcn*<sup>-/-</sup> (D and H) mice. The thick dentin and thin predentin (A and E; black arrow), lined by an odontoblast layer, surrounded the pulp in the *WT* incisor. Widened predentin was clearly observed in *Dspp*<sup>-/-</sup> mouse (B; arrow and F; \*). Biglycan deletion did not alter the widened predentin phenotype in *Dspp*<sup>-/-</sup> mouse (C; arrow and G; \*). The number of calcospherites was increased, thus forming an irregular mineralization front (G; red arrows). Most notably, decorin deletion restored widened predentin phenotype in *Dspp*<sup>-/-</sup> teeth (D and H; black arrows). am, ameloblasts; en, enamel; de, dentin; pd, predentin; od, odontoblasts. Bars = 100  $\mu$ m

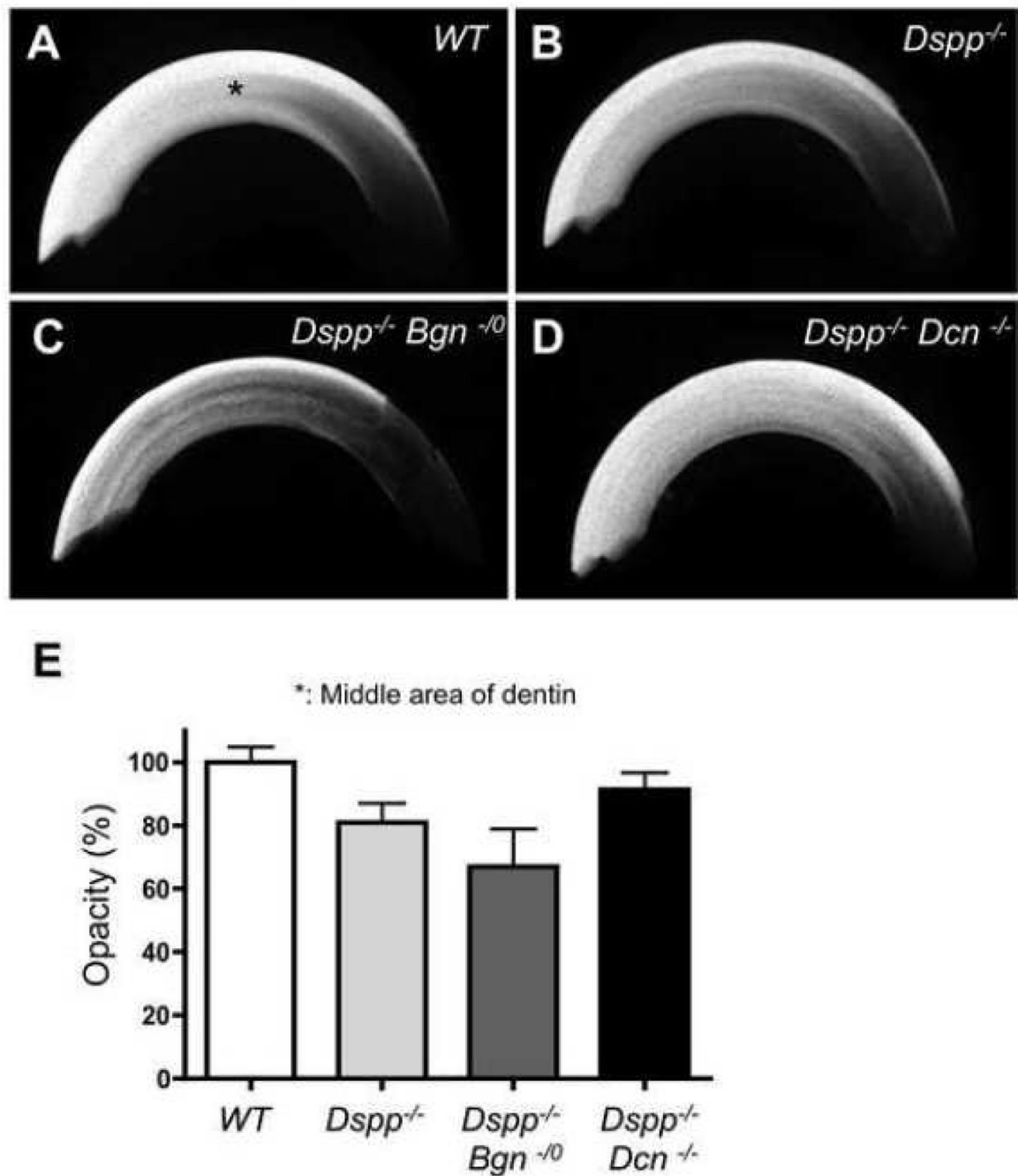


**Fig. 3. Altered X-ray opacity in upper incisors examined by microradiography** (A–D) Microradiographies taken from WT (A), *Dspp*<sup>-/-</sup> (B), *Dspp*<sup>-/-</sup> *Bgn*<sup>-/-</sup> (C) and *Dspp*<sup>-/-</sup> *Dcn*<sup>-/-</sup> (D) mice. The X-ray opacities in the labiolingually middle area of the incisors (\*) were compared for mineralization. The *Dspp*<sup>-/-</sup> dentin (B) showed a low opacity compared to WT (A). The *Dspp*<sup>-/-</sup> *Bgn*<sup>-/-</sup> showed the lowest opacity in the four groups (C). The *Dspp*<sup>-/-</sup> *Dcn*<sup>-/-</sup> demonstrated the increased opacity compared to *Dspp*<sup>-/-</sup> mice (D), suggesting that the lack of decorin rescued the DGI phenotypes in *Dspp*<sup>-/-</sup> mice (D). (E) Representative data of dentin opacity from WT, *Dspp*<sup>-/-</sup>, *Dspp*<sup>-/-</sup> *Bgn*<sup>-/-</sup> and *Dspp*<sup>-/-</sup> *Dcn*<sup>-/-</sup>. The statistical analysis was not applied to this data because of the small sample numbers.



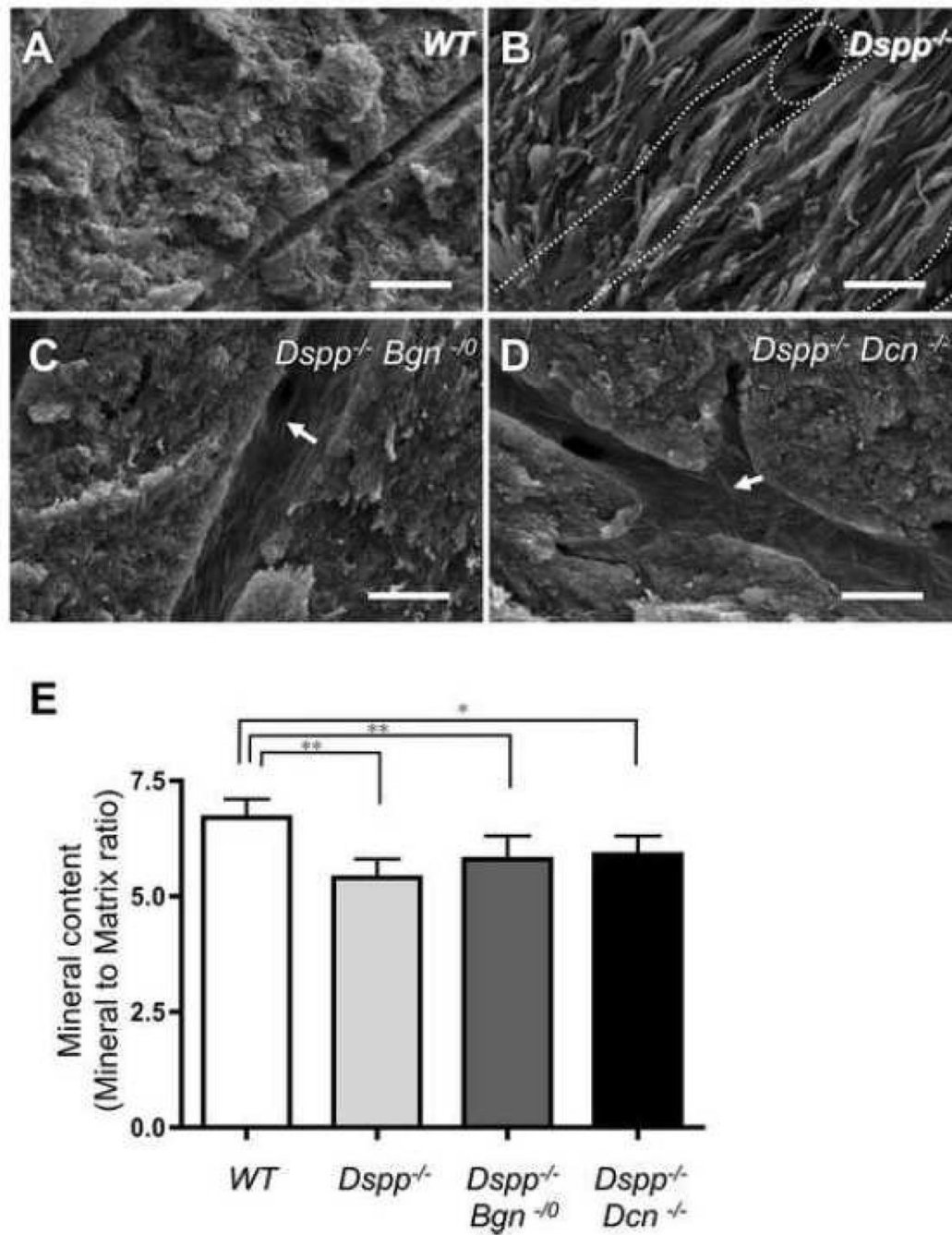


**Fig. 4. Characteristic comparison of fractured dentin surfaces by scanning electron microscopy (SEM) and quantitative analysis by Fourier transform infrared (FTIR) spectroscopy for the mineral contents (mineral to matrix ratio) in dentin**  
 (A–D) SEM analysis of incisors. Compared to the WT (A), the collagen fibrils could be clearly observed on the fractured dentin surface of the *Dspp*<sup>-/-</sup> mouse (B). The increased number of collagen fibrils was observed on the dentinal tubules and intertubular dentin from *Dspp*<sup>-/-</sup> *Bgn*<sup>-/-</sup> and *Dspp*<sup>-/-</sup> *Dcn*<sup>-/-</sup> samples (arrows in C and D), but much less than those of *Dspp*<sup>-/-</sup> (B). Dotted line; dentinal tubules. Bars = 1  $\mu$ m (E) Quantitative analysis of mineral contents in dentin by FTIR spectroscopy. The WT incisor demonstrated significantly higher mineral contents. \*,  $p < 0.05$ , \*\*,  $p < 0.01$ ,  $n = 9$ . The differences in mineral contents did not



show significant changes in  $Dspp^{-/-}$ ,  $Dspp^{-/-}Bgn^{-/0}$  and  $Dspp^{-/-}Dcn$  (E), although dentin hypomineralization appeared to be partially rescued by removing the biglycan or decorin from  $Dspp^{-/-}$  mice, based on the SEM observation (A–D).

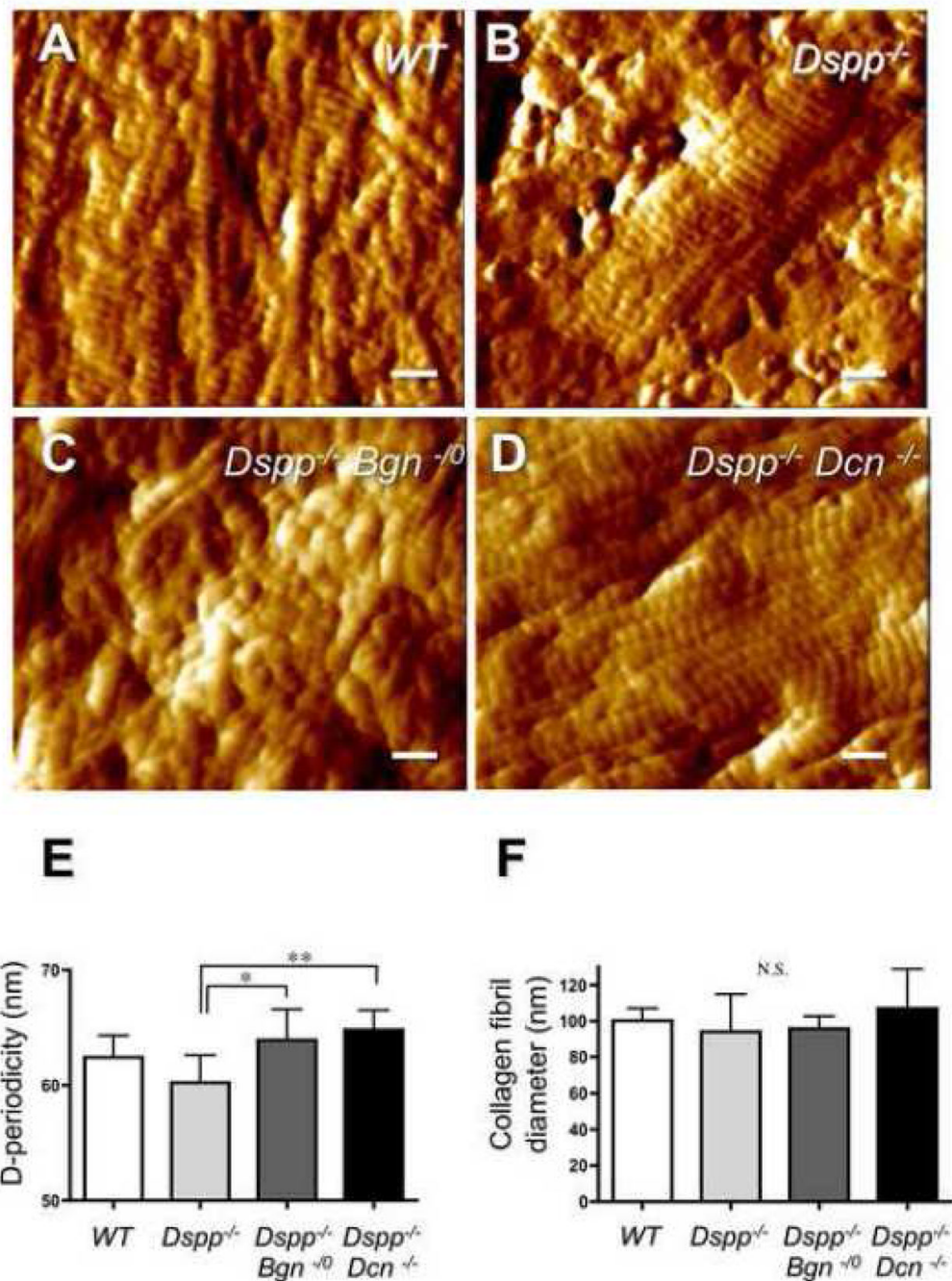


**Fig. 5. Collagen microstructures on the decalcified dentin surfaces observed by atomic force microscopy (AFM)**

(A) WT incisor after a 0.5 M EDTA treatment for 5 min. The whole surface was covered with the integral D-structure of collagens. (B) *Dspp*<sup>-/-</sup> samples treated by 0.5 M EDTA for 3 min. The collagen fibers and the D-structure could be revealed. (C) *Dspp*<sup>-/-</sup>*Bgn*<sup>-/-</sup> samples treated by EDTA for 3 min. *Dspp*<sup>-/-</sup>*Bgn*<sup>-/-</sup> samples also showed that several collagen fibrils were embossed on the dentin surface. (D) *Dspp*<sup>-/-</sup>*Dcn*<sup>-/-</sup> samples treated by EDTA for 3 min. The collagen fibrils were well-exposed due to the complete removal of mineralized material. Bars = 200 nm. (E) D-periodicity of the collagen fibrils. The periodicity of the D-structures on *Dspp*<sup>-/-</sup> incisor collagen fibers was significantly shorter than that of the *Dspp*<sup>-/-</sup>*Bgn*<sup>-/-</sup> or

*Dspp*<sup>-/-</sup>*Dcn*<sup>-/-</sup> collagen fibrils. \*; p<0.05, \*\*; p<0.01, n = 9. (F) The mean values of collagen fibril diameters. There was no significant difference in the collagen fibril diameter between the genotypes. The standard deviations in fibril diameter were bigger in the *Dspp*<sup>-/-</sup> (94.0 ± 20.9) and *Dspp*<sup>-/-</sup>*Dcn*<sup>-/-</sup> (107 ± 21.8) incisors (Fig. 5F), as compared with the *WT* (100.2 ± 6.8) and *Dspp*<sup>-/-</sup>*Bgn*<sup>-/0</sup>(95.7 ± 7.0). N.S.; not significant, n = 9.